Supplemental Figures

Supplemental Figure 1:

A: Minigene-specific, radioactive splicing sensitive RT-PCR and quantification using HeLa cells transfected with human and mouse U2AF35 minigenes or the empty vector (ev). GAPDH-specific radioactive RT-PCR was used as loading control. **B:** Splicing of human and mouse U2AF35 Q157R minigene in the presence of 5 µg/mL actinomycin D for different time points. Fold change Q157Rdel was quantified and normalized to DMSO (n=2). **C:** Distances between the Zn-coordinating cysteine (C) and histidine (H) residues in the ZnF2 of U2AF35wt, Q157R and Q157Rdel in Ångström. Distances were measured between the sulfur group of cysteine residues and the nitrogen group of the histidine residues.

Supplemental Figure 2:

A: Quantitative RT-PCR showing expression of U2AF35 relative to GAPDH in HEK293T cells transfected with control siRNA and U2AF35 siRNA. **B:** Cell proliferation was analyzed using a CFSE-based approach in the presence of U2AF35 variants following knockdown of endogenous U2AF35. Median CFSE signals were obtained 24, 48, 72 and 96 hours after transfection and normalized to 24 hours after transfection for each independent experiment (n=3). **C:** Cell cycle analysis in the presence of U2AF35 variants following knockdown of endogenous U2AF35 by flow cytometry. Percentage of cells in the indicated cell cycle stages are shown (n=3). **D+E:** Quantifications of splicing sensitive radioactive RT-PCRs for targets where Q157Rdel **(D)** can rescue and **(E)** cannot rescue U2AF35 knockdown. n≥3; *p<0,05; **p<0,01; ***p<0,001. **F:** U2AF35-knockdown was rescued by different ratios of U2AF35 wt to Q157Rdel plasmid while keeping the total plasmid amount constant to analyze a dominant negative effect of Q157Rdel. Alternative splicing was analyzed for two U2AF35-dependent target exons (n=2).

Supplemental Figure 3:

A: Validation of RNA-sequencing data with target exons using radioactive RT-PCRs from Figure 2 and Supplemental Fig. 2. **B:** 3’ splice site analysis of U2AF35 responsive exons identified in RNA-sequencing analysis. Target exons were grouped according to

their ability to be rescued by Q157P, Q157R and Q157Rdel and splice site consensus sequences were derived in the respective groups. **C:** Analysis of cassette exons with increased exon skipping upon U2AF35 knockdown that are unresponsive to wt U2AF35 rescue but responsive to mutant U2AF35 rescue. Overlap between Q157P, Q157R and Q157Rdel rescued targets and the 3` ss consensus motifs of unique targets are shown. **D:** Examples of splicing sensitive RT-PCRs for endogenous and minigene BCL2L12 exon 3 splicing quantified in Figure 3B.

Supplemental Figure 4:

A: Analysis of alternative splicing events in AML-patients with Q157R and Q157P mutations in comparison to patients with wt U2AF35. MISO was used to identify differential alternatively spliced event with a dPSI above 10% and Bayes factor ≥ 5. Moreover, events with confidence intervals diverging more than 10% from the calculated PSI value were eliminated. **B:** Depiction of 3' splice site motifs of cassette exons regulated in Q157R or Q157P patients. Shown are 3' splice sites of exons with increased or decreased exon inclusion compared to wt. **C:** Depiction of junction reads for the U2AF35 junction between exon 6 and exon 7 in Q157R and Q157P patients. **D:** Correlation of Q157P and Q157R dPSI values in cell culture and in patients taking into account a possible function of the Q157Rdel. dPSI of cell culture Q157P and Q157R were corrected with Q157Rdel values and plotted against the respective dPSI in patients.

Supplemental Figure 5:

A: Analysis of individual replicates of the cell line sequencing. A heatmap (left) shows the normalized Euclidean distances between samples, the dendrogram (right) shows clusters of related samples. The replicates cluster together with the exception of the siCTRL and the siU2AF35 wt U2AF35 rescue samples, which form a large cluster together, showing that the system recapitulates endogenous splicing. **B:** Analysis of individual replicates of the patient sequencing. Patients with the same mutation cluster together. Wild type patients form two larger clusters.

Supplemental Table 1

A: Number of mapped reads for HEK293T cells sequencing. **B:** U2AF35 knockdown affected cassette exons identified in sequencing of HEK293T cells. Shown are event names, gene names and IDs, percent splice in (PSI) values for all samples and categorization into rescue or non-rescue. Additional information about whether knockdown increases skipping and about the 3' splice site is given. **C:** BioSample numbers of patients of U2AF35 wt, Q157P and Q157R identified in the analyzed cohort (GSE67040) and used for further analysis. **D+E:** Differentially spliced events in patients with the Q157P **(D)** and Q157R **(E)** mutation compared to U2AF35 wt patients. Events are grouped in alternative 5' and 3' splice sites (A5SS or A3SS), mutually exclusive events (MXE), retained introns (RI) and skipped exons (SE). PSI and confidence intervals (ci) are shown for the mutant and the wt patients. Furthermore, the delta PSI, the corresponding Bayes factor and gene name and identification number are shown. **F:** Comparison of cassette exons in all three patient groups (wt, Q157P, Q157R). Same information as shown in (D+E). **G:** Overlap of events where knockdown increased skipping and wt U2AF35 was able to rescue in cells (from (B)) and events that were differentially spliced between at least one mutant and wt in patients (from (F)).**H:** List of Primers used in this study. Event type and alternative exon number of splicing events analyzed via RT-PCR are shown.

A

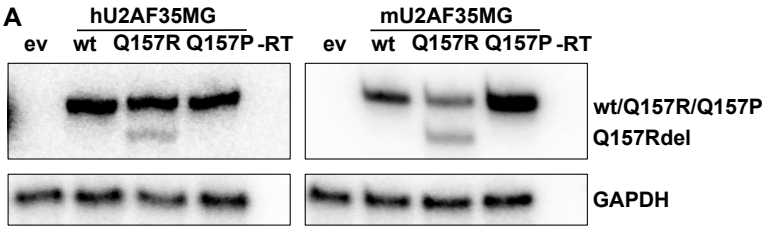

C

	wt	Q157R	Q157Rdel
C155-H173	3.57	3.84	3.44
C163-H173	3.42	3.67	3.96
C169-H173	3.43	3.48	3.07
C155-H163	4.04	3.97	4.14
C155-H169	3.86	3.76	4.13
C163-H169	4.06	4.11	5.60

B

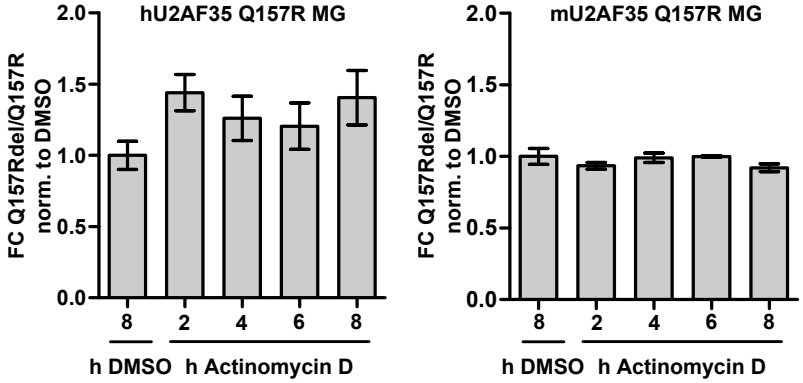

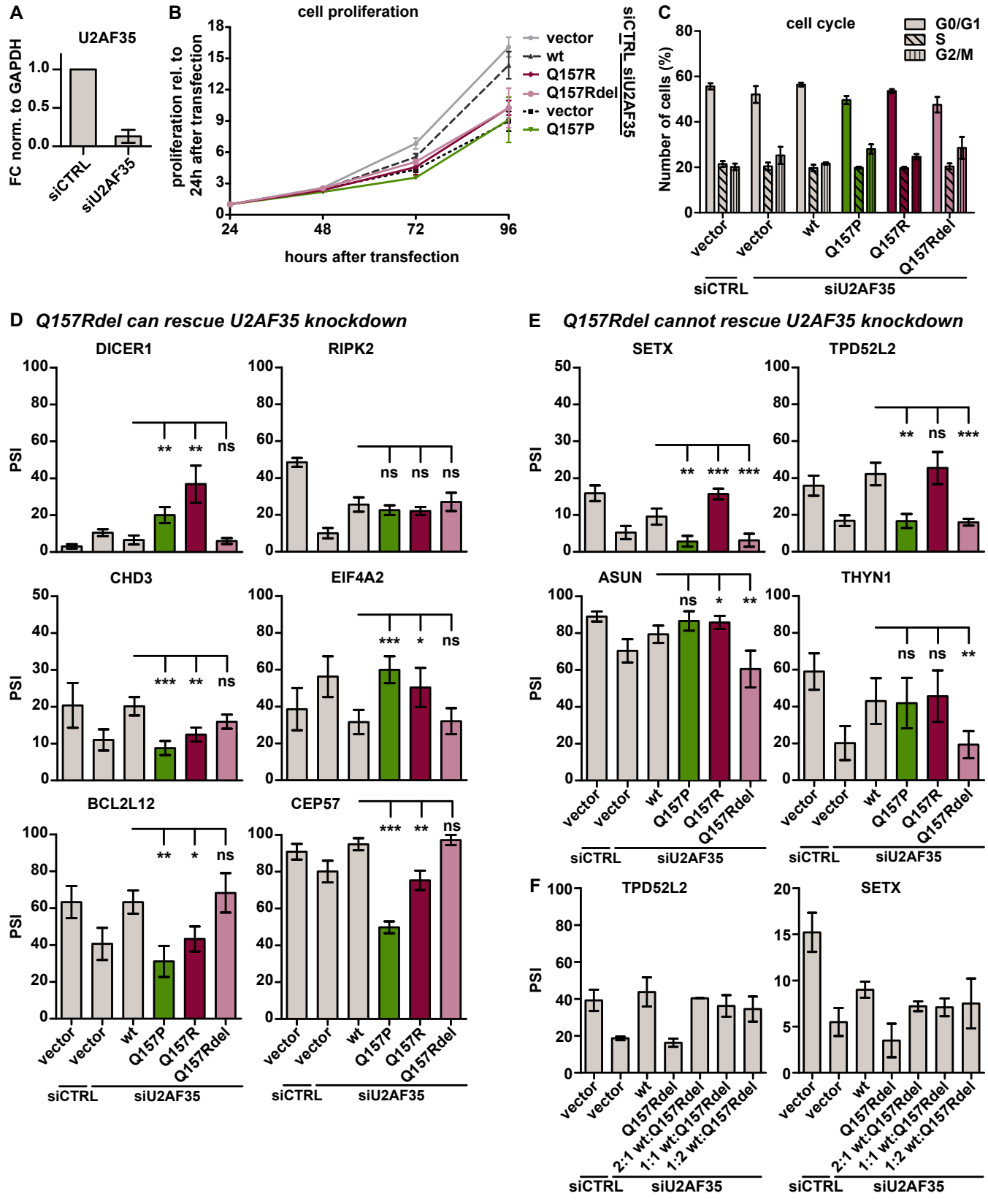
A
U2AF35
FC norm. to GAPDH
siCTRL
siU2AF35
B
cell proliferation
proliferation rel. to 24h after transfection
hours after transfection
vector
wt
Q157R
Q157Rdel
vector
Q157P
siCTRL siU2AF35
C
cell cycle
G0/G1
S
G2/M
Number of cells (%)
vector
vector
wt
Q157P
Q157R
Q157Rdel
siCTRL
siU2AF35
D Q157Rdel can rescue U2AF35 knockdown
DICER1
RIPK2
CHD3
EIF4A2
BCL2L12
CEP57
PSI
E Q157Rdel cannot rescue U2AF35 knockdown
SETX
TPD52L2
ASUN
THYN1
F
TPD52L2
SETX
Q157Rdel
2:1 wt:Q157Rdel
1:1 wt:Q157Rdel
1:2 wt:Q157Rdel

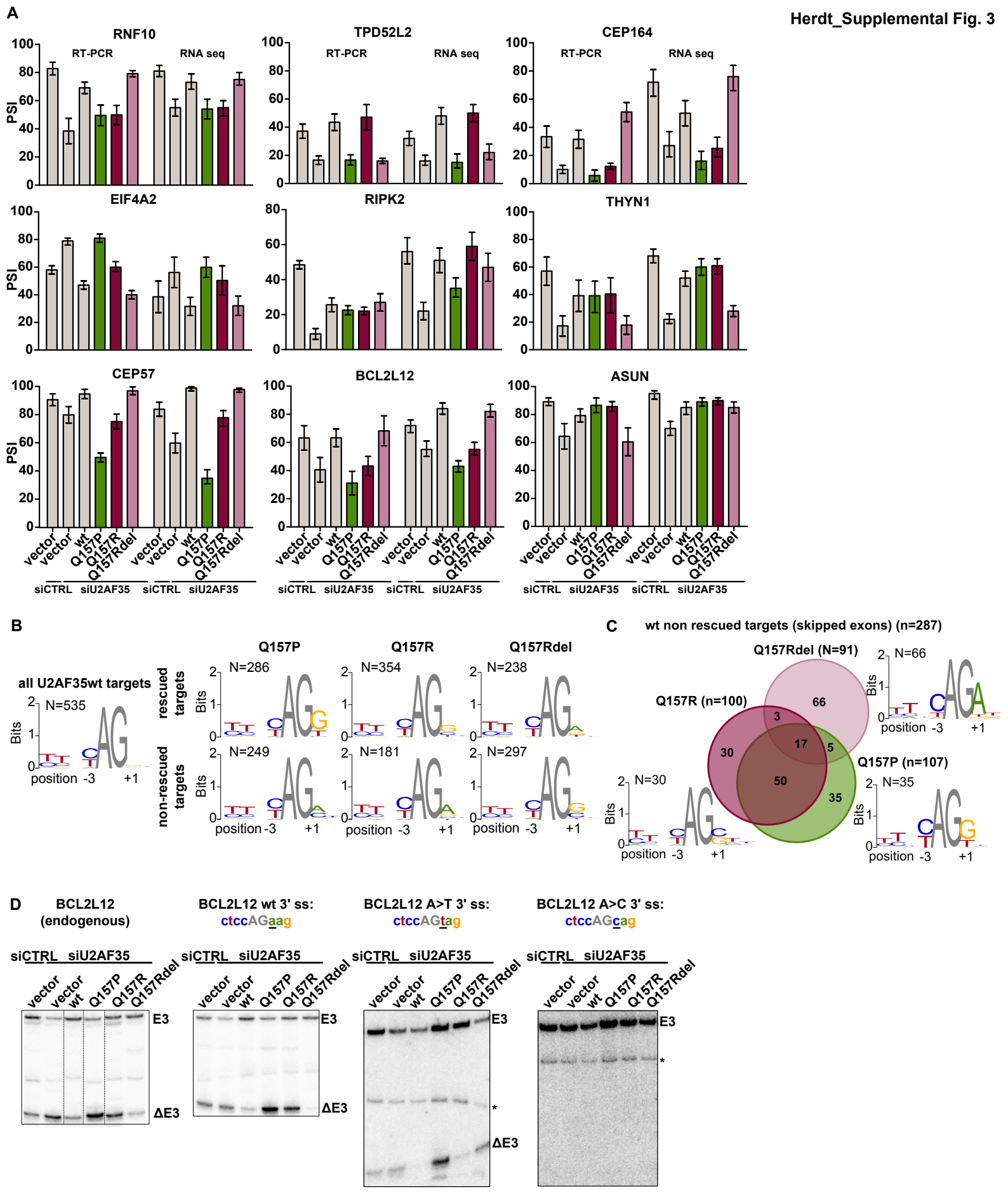
A
RNF10
TPD52L2
CEP164
EIF4A2
RIPK2
THYN1
CEP57
BCL2L12
ASUN
RT-PCR
RNA seq
PSI
vector
vector
wt
Q157P
Q157R
Q157Rdel
siCTRL
siU2AF35
B
all U2AF35wt targets
N=535
rescued targets
non-rescued targets
Q157P
Q157R
Q157Rdel
N=286
N=354
N=238
N=249
N=181
N=297
Bits
position -3 +1
C
wt non rescued targets (skipped exons) (n=287)
Q157Rdel (N=91)
Q157R (n=100)
Q157P (n=107)
66
3
17
5
30
50
35
N=66
N=30
N=35
D
BCL2L12 (endogenous)
BCL2L12 wt 3' ss:
ctccAGaag
BCL2L12 A>T 3' ss:
ctccAGtag
BCL2L12 A>C 3' ss:
ctccAGcag
siCTRL siU2AF35
E3
ΔE3
*

A

	Q157P patients	Q157R patients
alternative 3' ss	291	256
alternative 5' ss	192	160
mutually exclusive	104	114
retained intron	180	180
cassette exon	1107	1139
∑ differentially spliced to wt	**1874**	**1849**

B

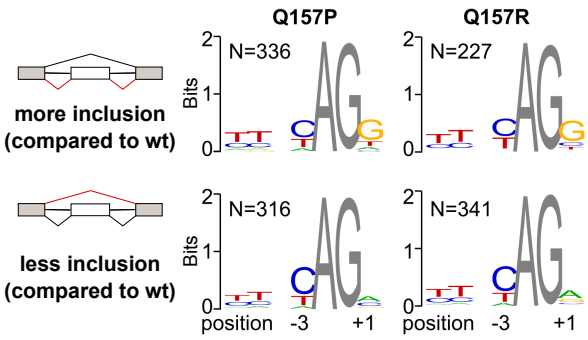

C

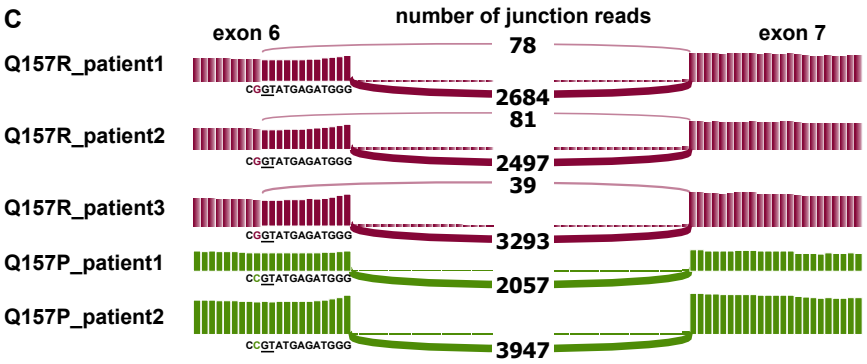

D

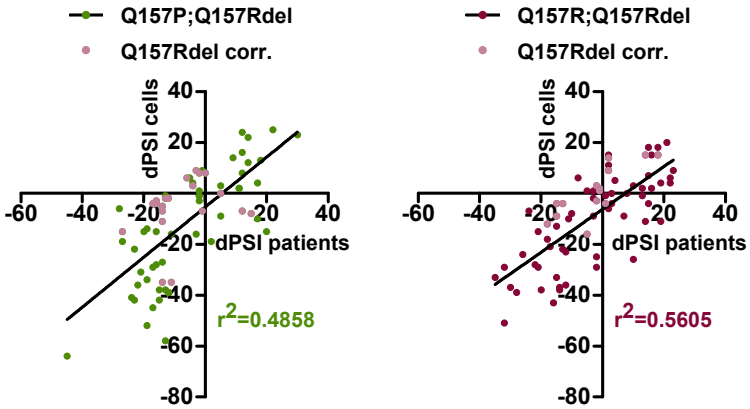

A

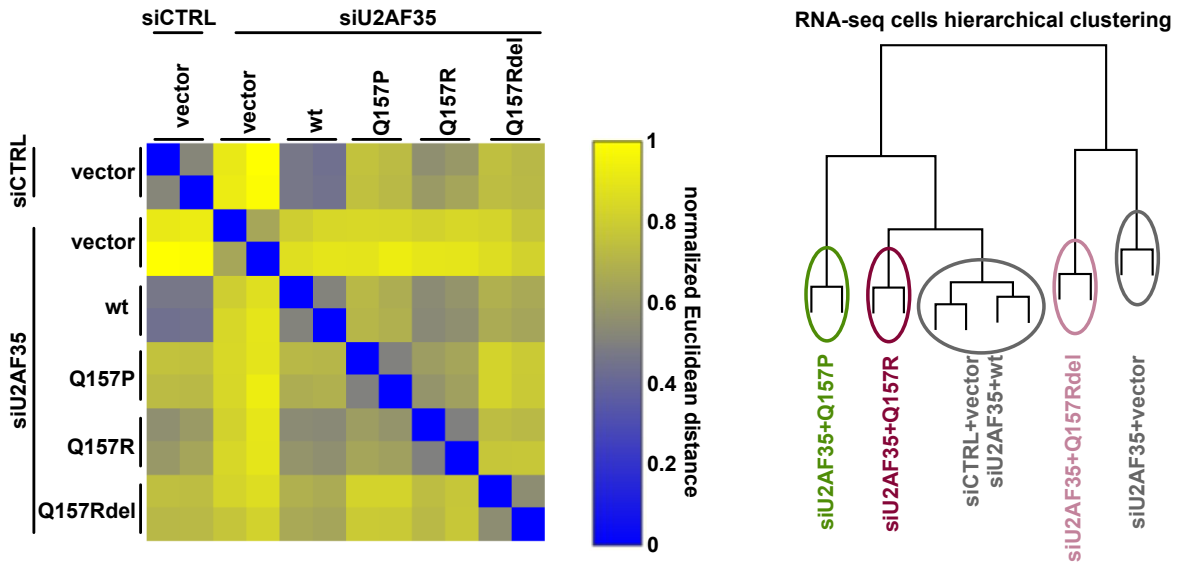
RNA-seq correlation cells
siCTRL
siU2AF35
vector
vector
wt
Q157P
Q157R
Q157Rdel
siCTRL
siU2AF35
vector
vector
wt
Q157P
Q157R
Q157Rdel
1
0.8
0.6
0.4
0.2
0
normalized Euclidean distance
RNA-seq cells hierarchical clustering
siU2AF35+Q157P
siU2AF35+Q157R
siCTRL+vector
siU2AF35+wt
siU2AF35+Q157Rdel
siU2AF35+vector

B

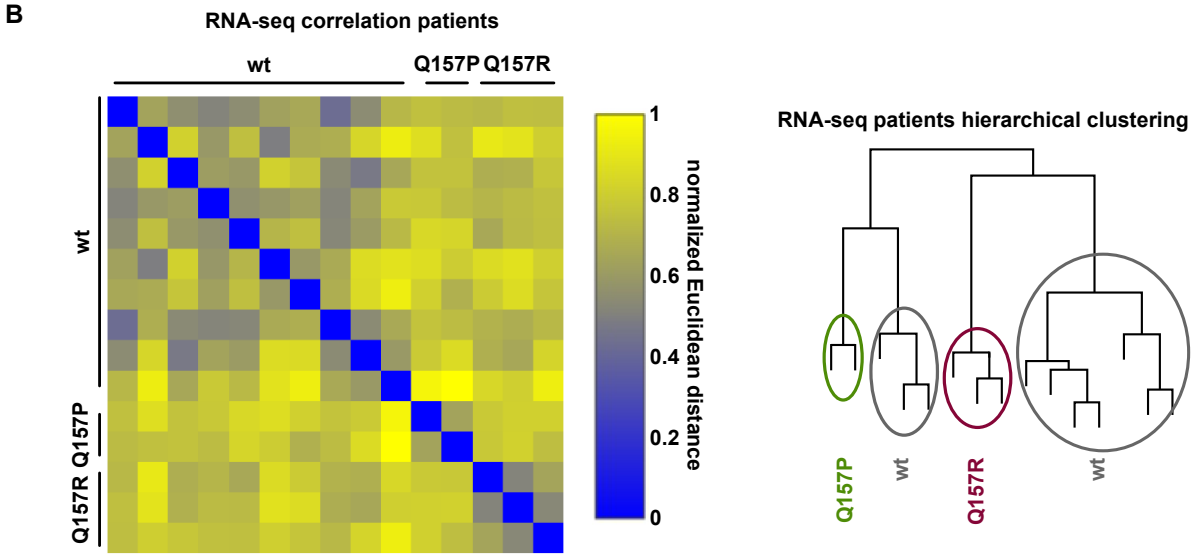
RNA-seq correlation patients
wt
Q157P
Q157R
wt
Q157P
Q157R
1
0.8
0.6
0.4
0.2
0
normalized Euclidean distance
RNA-seq patients hierarchical clustering
Q157P
wt
Q157R
wt